4
Model-based Control

Sebastian Engell, Gregor Fernholz, Weihua Gao, and Abdelaziz Toumi

4.1
Introduction

As explained in several chapters of this volume, rigorous process models can be used to optimize the design and the operating parameters of chemical processing plants. However, optimal settings of the parameters do not guarantee optimal operation of the real plant. The reasons for this are the inevitable plant-model mismatches, the effects of disturbances, changes in the plant behavior over time, etc. Usually not even the constraints on process or product parameters are met at the real plant if operating parameters that were obtained from offline optimization are applied.

The only effective way to cope with the effect of plant-model mismatch, disturbances etc. is to use some sort of feedback control. Feedback control means that (some of) the degrees of freedom of the plant are modified based on the observation of measurable variables. These measurements may be performed quasicontinuously or with a certain sampling period, and accordingly the operation parameters (termed inputs in feedback control terminology) may be modified in a quasicontinuous fashion or intermittently. Often, key process parameters cannot be measured online at a reasonable cost. One important use of process models in process control is the model-based estimation of such parameters from the available measurements. This topic has been dealt with in the previous chapter. In this chapter, we focus on the use of rigorous process models for feedback control by model-based online optimization.

Feedback control can be combined with model-based optimization in several different ways. The simplest, and most often used, approach is to perform an offline optimization and to divide the degrees of freedom into two groups. The variables in the first group are applied to the real process as they were computed by the offline optimization. The variables in the second group are used to control some other variables to the values which resulted from the offline optimization, e.g., requirements on purities are met by controlling the product concentration by manipulating the feed rate to a reactor or the reflux in a distillation column. In the design of these feedback controllers, dynamic plant models are used, in most cases obtained from a line-

Computer Aided Process and Product Engineering. Edited by Luis Puigjaner and Georges Heyen

ISBN: 3-527-30804-0

arization of the rigorous model around the optimal operating regime or process trajectory. If nonlinear process models are available from the design stage, these models can be used directly in model-based control schemes. This leads to nonlinear model-predictive control (NMPC) where the future values of the controlled variables are predicted over a finite horizon (the prediction horizon) using the model, and the future inputs are optimized over a certain horizon (the control horizon). The first inputs' values are applied to the plant. Thereafter, the procedure is repeated, taking new measurements into account. A major advantage of this approach is the ability to include process constraints in the optimization, thus exploiting the full potential of the plant and the available actuators (pumps, valves) and respecting operating limits of the equipment. In Section 4.2, NMPC around a precomputed trajectory of the process is presented in more detail and its application to a reactive semibatch distillation process is discussed.

When closed-loop control is used to track a precomputed trajectory and the controllers perform satisfactorily, the process is kept near the operating point that was computed as the optimal one offline. Those variables which are under feedback control track their precomputed set-point even in the presence of disturbances and plant-model mismatch. However, the overall operation will in general no longer be optimal, because the precomputed operating regime is optimal for the nominal plant model, but not for the real plant.

As an extension of this concept, feedback control can be combined with model adaptation and reoptimization. At a lower sampling rate than the one used for control, some model parameters are adapted based upon the available measurements. After the model has been updated, it is used for a reoptimization of the operating regime. The new settings can be implemented directly or be realized by feedback. In Section 4.3, such a control scheme is presented for the example of batch chromatographic separations, including experimental results.

A serious problem in practice is structural plant-model mismatch. This means that an adaptation of the model parameters, even for an infinite number of noise-free measurements, will not give a model that accurately represents the real process. Therefore if the structurally incorrect model is used in optimization, the resulting operating parameters will not be optimal; often, not even the constraints will be met by the real process unless the constrained variables are under feedback control with some safety margin that reflects the attainable control performance, which again causes a suboptimal operation.

A solution to the problem of plant-model mismatch is the use of optimization strategies that incorporate feedback directly, i.e., use the information gained by online measurements not only to update the model but also to modify the optimization problem. In Section 4.4, this idea is presented in detail and the application to batch chromatography is used to demonstrate its potential.

NMPC involves online optimization on a finite horizon based upon a nonlinear plant model. This approach can be employed not only to keep some process variables at their precomputed values or make them track certain trajectories, but also to perform online predictive optimization of the plant performance. Bounds, e.g., on product specifications, can be included in the formulation as constraints rather than set-

ting up a separate feedback control layer to meet the specifications at the real plant. In this spirit, the problem of controlling quasicontinuous (simulated moving bed) chromatographic separations is formulated in Section 4.5 as an online optimization problem, where the measured outputs have to meet the constraints on the product purities but the optimization goal is not tracking of a precomputed trajectory, but optimal process operation.

4.2
NMPC Applied to a Semibatch Reactive Distillation Process

4.2.1
Formulation of the Control Problem

In NMPC, a process model is used to predict the future process outputs $\hat{\mathbf{y}}$ over a fixed prediction time horizon H_p for given sequences of H_r changes of the manipulated variables $\mathbf{u}$. The aim of the controller is to minimize a quadratic function of the deviation between the process outputs $\hat{\mathbf{y}}$ and their desired trajectories $\mathbf{y}^{ref}$ as well as of the changes of the manipulated variables. The control move at the sampling point $k+1$ is given by the optimization problem Eq. (1). The parameters $\boldsymbol{\gamma}_{ij}$ and $\boldsymbol{\lambda}_{ij}$ allow scaling the controlled and manipulated variables and shifting the weight either on good setpoint tracking or on smooth controller actions. Bounds on the manipulated variables can be enforced by using sufficiently large penalties $\boldsymbol{\lambda}_{ij}$ or by adding inequality constraints (Eq. (2)) to the optimization problem Eq. (1):

$$\min_{\mathbf{u}_{k+1},\ldots,\mathbf{u}_{k+H_r}} \left\{ \sum_{i=1}^{H_p} \sum_{j=1}^{m} \gamma_{ij} \left(y_{j,k+i}^{ref} - \hat{y}_{j,k+i} \right)^2 + \sum_{i=1}^{H_r} \sum_{j=1}^{r} \lambda_{ij} \left(u_{j,k+i}^{ref} - u_{j,k+j} \right)^2 \right\} \tag{1}$$

$$\mathbf{u}_j^{min} \leq \mathbf{u}_{k+j} \leq \mathbf{u}_j^{max} \quad \forall j = 1, \ldots, H_r . \tag{2}$$

If the control scheme is applied to a real plant, plant-model mismatch or disturbances will lead to differences between the predicted and the real process outputs. Therefore a time-varying disturbance model, as proposed by Draeger et al. (1995), is included in the process model. The formal representation of the complete model that is used by the model predictive controller is

$$\hat{y}_{(k+i)} = \mathbf{y}_{(k+i)}^{model} + \mathbf{d}_{k,i} \quad \forall i = 1, \ldots, H_p \tag{3}$$

where $\mathbf{d}_{k,i}$ denotes the estimated disturbances, y_k^{model} denotes the model outputs given by the physical process model, and $\hat{y}_k$ the model prediction of the controller used in the optimization problem (1). The disturbances $\mathbf{d}_{k,i}$ are recalculated at every time k for each time step i. The process model is simulated from time k–i until time k taking into account the actual control actions giving the model outputs $\mathbf{y}^{model}(k|k\text{-}i)$. The errors $\mathbf{e}_{k,i}$ computed as the differences between the measurements y_k^{meas} and the model outputs $\mathbf{y}^{model}(k|k-i)$:

$$\mathbf{e}_{k,i} = \mathbf{y}_k^{\text{meas}} - \mathbf{y}^{\text{model}}(k \mid k-i). \tag{4}$$

The new estimates of the disturbances are calculated by a first order filter:

$$\mathbf{d}_{k,i} = \alpha \mathbf{e}_{k,i} + (1-\alpha)\mathbf{d}_{k-1,i}. \tag{5}$$

4.2.2 The Methyl Acetate Process

Methyl acetate is produced from acetic acid and methanol in an esterification reaction. The conventional process consists of a reactor and a complex distillation column configuration, while using reactive distillation, high purity methyl acetate can be produced in a single column (Agreda et al. 1990). The reaction can either by catalyzed homogeneously by sulfonic acid or heterogeneously using a solid catalyst. The latter avoids material problems caused by the sulfonic acid as well as the removal of the catalyst at the end of the batch. This process is investigated here. A scheme of the process is shown in Figure 4.1.

The column consists of three parts. Two structured catalytic packings of 1 m height are located in the lower part of the column while the upper part contains a noncatalytic packing. Methanol is filled into the reboiler before the beginning of the batch and heated until the column is filled with methanol. Acetic acid is fed to the column above the reactive section. Since acetic acid is the highest boiling component, it is necessary to feed it above the catalytic packing in order to ensure that both raw materials are present in the catalytic area in sufficient concentrations. The upper section purifies the methyl acetate. The azeotropes of the mixture are overcome because water and acetic acid are present in the stream that enters the separation stages. The plant considered here is a pilot plant in the Department of Biochemical and Chemical Engineering at Universität Dortmund. A batch run takes approximately 17 h.

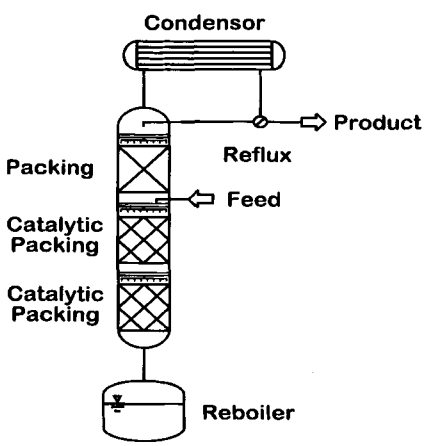

Figure 4.1 Scheme of the semibatch column

A more detailed description of the process and a rate-based model and its validation are presented in Kreul et al. (1998) and Noeres (2003). The latter pointed out that for this process the accuracy of a rate-based model is not significantly higher than that of an equilibrium stage model, and thus the equilibrium stage model was used to determine the optimal operation of the process (Fernholz et al. 2000) and as a basis for controller design. Mass and energy balances for all parts of the plant result in a differential-algebraic equation system consisting of more than 2000 equations. The main assumptions in the model are:

- The structured packings can be treated as a number of theoretical plates using the HETP-value (height equivalent to theoretical plate).
- The vapor and the liquid phase are in thermodynamic equilibrium.
- All chemical properties depend on the temperature and the composition.
- The phase equilibrium is calculated using the Wilson equations. The dimerization of acetic acid in the vapor phase is taken into consideration.
- The reaction kinetics are formulated by a quasihomogeneous correlation.
- The pressure drop of the packing is calculated by the equation of Máckowiak (1991).
- The hold-up of the packing is determined by an experimentally verified correlation.
- Negligible vapor hold-up.
- Ideal vapor behavior.
- Constant molar hold-up in the condenser.
- The dynamics of the tray hydraulics and the liquid enthalpy are taken into consideration.

The aim of the controller is to ensure the tracking of the optimal trajectory in the presence of model inaccuracies and disturbances acting on the process.

4.2.3 Simplified Solution of the Model Equations

Generally, any process model can be used to predict the future process outputs $\hat{\mathbf{y}}_{k+1,n}$ as long as the model is sufficiently accurate. A straightforward approach would be to use the same model that was used to calculate the optimal operation. Unfortunately the integration of this differential algebraic model is too time-consuming to solve the optimization problem given by Eqs. (1) and (2) within one sampling interval. Thus, a different model had to be developed to make sure that the solution of Eqs. (1) and (2) is found between two sampling points.

The physical process model is based on heat and mass balances resulting in a set of differential equations. A large number of algebraic equations is needed to calculate the physical properties, the phase equilibrium, the reaction kinetics and the tray hold-ups, as well as the connections between the different submodels. Various numerical packages are now available to solve large differential-algebraic equation (DAE) systems like gPROMS (1997) or the Aspen Custom Modeler (ACM). Even

though they are designed to solve large and sparse DAEs in an efficient way, general-purpose solvers do not take advantage of the mathematical structure of a special problem. Our aim was to find a way to reduce the numerical effort required to calculate the solution of the DAE system which describes the reactive distillation process.

The main idea is to split up the equation system into a small section that is treated by the solver in the usual manner and a large subsystem containing mainly the algebraic equations. An independent solver that communicates with the DAE solver calculates the solution of this subsystem. Generally, this sequential approach may not be advantageous since the solution of the algebraic part must be provided in each step of the iteration of the DAE solver. It will only be superior if the solution of the second part is calculated in a highly efficient way. Therefore an analysis of the system equations for one separation tray is given in the sequel. Similar considerations can be easily made for the reactive trays as well as the other submodels of the process.

The core of the model for each separation tray consists of the mass balances of the components (Eq. (6)) the heat balance (Eq. (7)), and the constitutive equation for the liquid mole fractions (Eq. (8)):

$$\frac{\mathrm{d}}{\mathrm{d}t}(x_i N) = L^{\mathrm{in}} x_i^{\mathrm{in}} - L^{\mathrm{out}} x_i + V^{\mathrm{in}} y_i^{\mathrm{in}} - V^{\mathrm{out}} y_i, \tag{6}$$

$$\frac{\mathrm{d}}{\mathrm{d}t}(h_{\mathrm{lig}} N) = L^{\mathrm{in}} h_{\mathrm{liq}}^{\mathrm{in}} - L^{\mathrm{out}} h_{\mathrm{liq}} + V^{\mathrm{in}} h_{\mathrm{vap}}^{\mathrm{in}} - V^{\mathrm{out}} h_{\mathrm{vap}}, \tag{7}$$

$$1 = \sum x_i. \tag{8}$$

In addition to the core Eqs. (6)–(8), empirical correlations are used to calculate the molar hold-ups of the trays (Eq. (9)), the liquid enthalpy (Eq. (10)), the vapor enthalpy (Eq. (11)), and the density (Eq. (12)):

$$N = c\rho^{2/3} L^{1/3}, \tag{9}$$

$$h_{\mathrm{liq}} = f_1(x_i, T), \tag{10}$$

$$h_{\mathrm{vap}} = f_2(y_i, T), \tag{11}$$

$$\rho = f_3(x_i, T). \tag{12}$$

Finally the phase equilibrium is calculated by using a four-parameter Wilson activity coefficient model for the liquid phase and a vapor-phase model which takes into consideration the dimerization of the acetic acid in the vapor phase (Noeres 2003). This phase equilibrium model (Eq. (13)) is an implicit set of equations in contrast to Eqs. (9)–(12) which are explicit functions of the composition and the temperature.

$$y_i = \frac{x_i \cdot \gamma_i \cdot p_i^0}{\varphi_i \cdot p}, \tag{13a}$$

$$1 = \sum y_i. \tag{13b}$$

Even though the formal description of Eqs. (9)–(13) feigns that its size is similar to the core model Eqs. (6)–(8), the opposite is true. Owing to the necessity of introducing a lot of auxiliary variables, especially for the phase equilibrium, Eqs. (9)–(13) make up the largest part of the overall system. Thus the idea is to move as many algebraic equations as possible, especially the parts containing the auxiliary variables, from the part which is handled by the DAE solver to an additional solver that exploits the mostly explicit structure of the equations. The DAE solver used in this work is DASOLVE, a standard solver in gPROMS for stiff DAEs (gPROMS, 1997). The proposed architecture of the algorithm is shown in Figure 4.2.

The main task of the external software is to solve the implicit phase equilibrium Eq. (13a,b) in an efficient manner. Solving Eq. (13a,b) for given pressure and liquid composition means to find the temperature T such that condition Eq. (13b) is fulfilled for the values calculated by Eq. (13a). Thus, the phase equilibrium calculation can be treated as solving a nonlinear equation with one unknown variable. Once Eq. (13a) and Eq. (13b) are solved, the remaining variables can be calculated straightforwardly by the explicit Eqs. (9)–(12). All values are passed back from the DAE solver via the foreign object interface.

In order to minimize the number of equations handled by the DAE-solver, the dynamics of the tray hold-up N and the liquid enthalpy h_{liq} were neglected. This causes deviations between the original model and the model with neglected dynamics. Several case studies were performed to check the differences between the original model and the model with neglected dynamics. In many cases the predictions of both models can hardly be distinguished. In some cases, however, noticeable differences in the dynamic behaviors result. These inaccuracies have to be handled by the disturbance estimation of Eqs. (3)–(5). By applying this scheme to the complete column model, the time required to calculate the solution for typical model predictive control scenarios could be reduced by a factor of 6–10.

The use of a simplified model and the special solution algorithm enable the online solution of the optimal control problem of Eqs. (1)–(3). The optimization algorithm L-BFGS-B of Byrd et al. (1994) is used to solve the optimization problem. This code solves nonlinear optimization problems with simple bounds on the decision variables and ensures a decrease of the goal function in each iteration step. The user of this code has to supply the values of the goal function as well as its derivatives with respect to the decision variables. The value of the cost function is calculated by integrating the model, the derivatives are obtained by perturbation. Using perturbations offers the opportunity to parallelize the calculation. Within a sampling period of

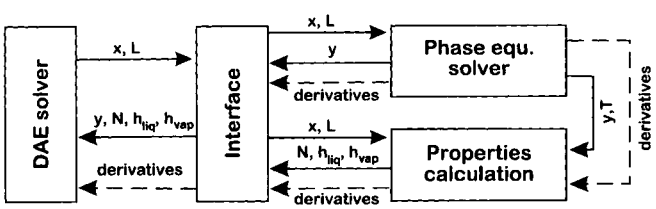

Figure 4.2 Scheme of the algorithm

6 min, about 100 function and gradient evaluations can be performed. The maximal number of function and gradient evaluations which were needed for the cases investigated was 33. Thus, the algorithm is able to find the optimal solution within the sampling time.

4.2.4 Controller Performance

The analysis of Fernholz et al. (1999a) showed that a suitable control structure for this process is to control the concentrations of methyl acetate and water in the product stream by the reflux ratio and the heat duty of the reboiler. At our pilot plant, NIR (near infrared spectroscopy) measurements of the product concentrations are available. The nonlinear model predictive controller was tested in several simulation cases. Here the original model is used as the simulated process, whereas the simplified model is used in the controller. In order to explore the benefits of the nonlinear controller, a linear controller was designed as well (Engell and Fernholz 2003). The linear controller was chosen based on an averaged linear model calculated from several linear models which were obtained by linearization of the nonlinear model at several points on the optimal trajectory. The controller design was done using the frequency response approximation technique (Engell and Müller 1993). The details of the linear controller design are beyond the scope of this book, they can be found in Fernholz et al. (1999b).

The parameters of the cost function in Eq. (1) were chosen such that deviations of both controlled variables give the same contribution to the objective functions. Additional bounds on the manipulated variables were added. The reflux ratio is physically bounded by the values 0 and 1, while the heat duty is bounded to a lower value of 1 kW and an upper one of 8 kW to ensure proper operation of the column. In order to avoid undesired abrupt changes of the manipulated variables, small penalties on these changes were added. The values of the penalty parameters λ_{ij} were selected in a way that large changes are possible for large deviations of the controlled variables but are unfavorable if they are close to their set-points[1]. Preliminary work on the model predictive control of this process had shown that the choice of a control horizon of $H_r = 2$ and of a prediction horizon of $H_p = 5$ gave good results. The closed loop responses for a set-point change of the methyl acetate concentration from a mole fraction of 0.8 down to 0.6 and back to 0.8 are shown in Figure 4.3. The use of the nonlinear controller reduces the time required to decrease the methyl acetate concentration drastically. The price that has to be paid for this reduction is a larger deviation of the water concentration. For the set-point change back to the original value, the differences between the two controllers are small.

Next, the performance of both controllers was checked for set-points of methyl acetate and water which force the process into a region where a sign change of the static gain occurs. If the set-points of the mole fractions of methyl acetate and water are

1 The value of all λ_{ij} is 0.01, while γ is set to one. The physical units of the controlled variables are mole mole^{-1}, the reflux ratio is dimensionless and the heat duty is given in kilowatts.

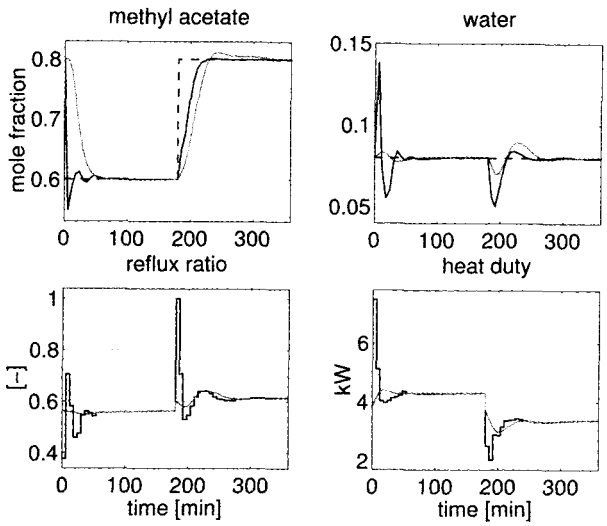

Figure 4.3 Methyl acetate set-point tracking. *Black:* nonlinear controller; *grey:* linear controller

changed simultaneously to 0.97 and 0.02 respectively, both controllers drive the process in the correct direction (Figure 4.4), but only the nonlinear controller is able to track both concentrations accurately. If the set-points are set back to their original values, the linear controller becomes unstable while the nonlinear controller works properly.

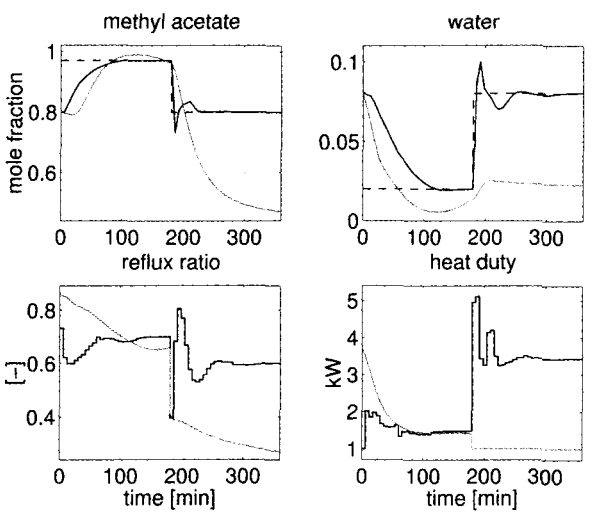

Figure 4.4 Set-point tracking in a region of a sign change of the static gain. *Black:* nonlinear controller; *grey:* linear controller

4.2.4.1

Disturbance Rejection

The main goal of the controller is to track the optimal trajectory of the process in the case of disturbances and plant-model mismatch. In the case of an accurate model and the absence of disturbances, no feedback controller would be necessary. Thus, two disturbances are imposed on the process during the simulation to test the disturbance rejection capabilities of the controllers.

First the influence of disturbances of the heat supply is considered. After 200 min the heat supply is decreased by 0.7 kW (which is about 20 % of the nominal value), set back to its nominal value at $t = 300$ min and increased by 0.7 kW at $t = 550$ min until it is again reset to the nominal value at $t = 700$ min. The simulation results for both controllers are depicted in Figure 4.5. The nonlinear controller rejects the disturbance much faster than the linear controller, especially for the product methyl acetate.

The second disturbance investigated is a failure of the heating system of the column. In order to minimize heat losses across the column surface, the plant is equipped with a supplementary heating system. A malfunction of this system will change the heat loss across the surface. The heat loss is increased by 50 W per stage, set back to 0 and decreased by 50 W per stage at the same times at which the disturbances of the heat duty were imposed before. The simulation results in Figure 4.6 show that the nonlinear controller rejects this disturbance more efficiently than the linear controller. Thus, the disturbance rejection can be significantly improved by using the nonlinear predictive controller.

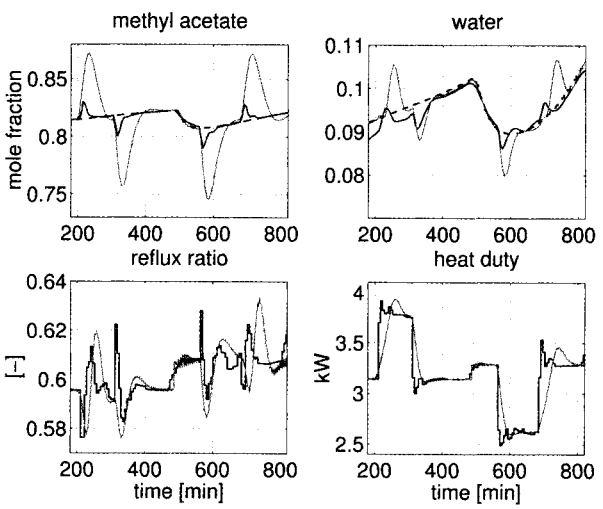

Figure 4.5 Rejection of a disturbance in the heat supply. *Black*: nonlinear controller; *grey*: linear controller; *dashed*: optimal trajectory

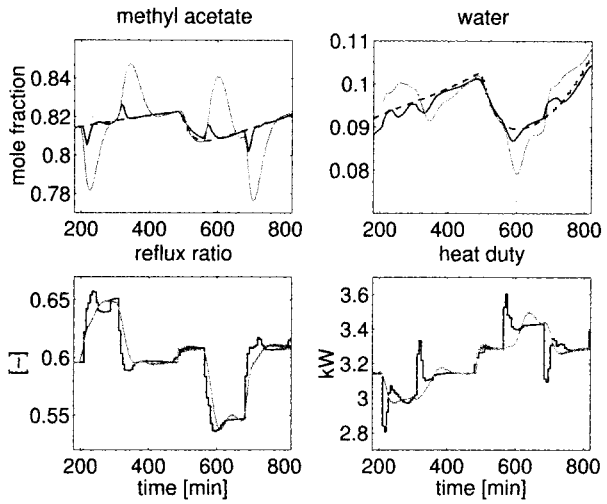

Figure 4.6 Rejection of a disturbance in the heat loss. *Black*: nonlinear controller; *grey*: linear controller; *dashed*: optimal trajectory

4.2.5

Summary

In this section, we presented the principle of NMPC to track a precomputed trajectory of a complex process and discussed the application to a semibatch reactive distillation column. Neglecting the dynamics of the molar hold-ups and of the enthalpies enabled splitting up the original DAE system into a small DAE part, which is treated by the numerical simulator, and an algebraic part, which is solved by an external algorithm. This approach reduced the time needed to solve the model equations by a factor of 6–10. These reductions made the use of a process model that is based on heat and mass balances possible for a model predictive controller.

The resulting nonlinear controller showed superior set-point tracking properties compared to a carefully designed linear controller. The nonlinear controller is able to track set-points that lie in regions where the process shows sign changes in the static gains and any linear controller becomes unstable. The nonlinear controller rejects disturbances faster than the linear controller. Moreover, since the nonlinear controller makes use of a model the range of validity of which is not restricted to a fixed operating region in contrast to the linear one, the nonlinear controller might be used for different trajectories giving more overall flexibility. The superior performance of the controller is due to the fact that a nonlinear process model is used. On the other hand, its stability and performance depend on the accuracy of the rigorous process model. If, e.g., the change of the gain of the process (which is caused by the fact that the product purity is maximized for certain values of reflux and heat duty) occurs for different values of the reflux and the heat duty than predicted by the model, the controller may fail to stabilize the process.

4.3
Control of Batch Chromatography Using Online Model-based Optimization

4.3.1
Principle and Optimal Operation of Batch Chromatography

The chromatographic separation is based on the different adsorptivities of the components to a specific adsorbent which is fixed in a chromatographic column. The most widespread process, batch chromatography, involves a single column which is charged periodically with pulses of the feed solution. These feed injections are carried through the column by pure desorbent. Owing to different adsorption affinities, the components in the mixture migrate at different velocities and therefore they are gradually separated. At the outlet of the column, the purified components are collected between cutting points, the locations of which are decided by the purity requirements on the products (Figure 4.7).

For a chromatographic batch process with given design parameters (combination of packing and desorbent, column dimensions, maximum pump pressure), the determination of the optimal operating regime can be posed as follows: a given amount (or flow) of raw material has to be separated into the desired components at minimal cost while respecting constraints on the purities of the products. The operation cost may involve the investment into the plant and the packing, labor and solvent cost, the value of lost material (valuable product in the nonproduct fractions) and the cost of the further processing, e.g., removal of the solvent. The free operating parameters are:

- the throughput of solvent and feed material, represented by the flow rate Q or the interstitial velocity u, constrained to the maximum allowed throughput which in turn is limited by the efficiency of the adsorbent or the pressure drop;
- the injection period t_{inj}, representing the duration of the feed injection as a measure of the size of the feed charge;
- the cycle period t_{cyc}, representing the duration from the beginning of one feed injection to the beginning of the next;
- the fractionating times.

The mathematical modeling of single chromatographic columns has been extensively described in the literature by several authors, and is in most cases based on differential mass balances (Guiochon 2002). The modeling approaches can be classified by the physical phenomena they include and thus by their level of complexity. Details

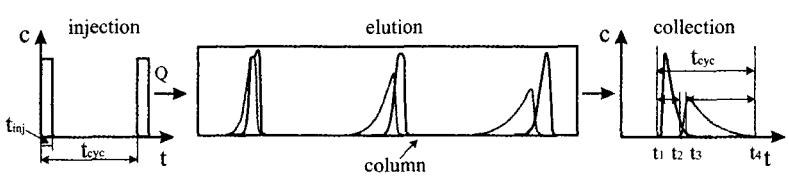

Figure 4.7 Principle of batch chromatography

on models and solution approaches can be found e.g., in (Dünnebier and Klatt 2000). The most general one-dimensional model (ignoring radial inhomogeneities) is the general rate model (GRM)

$$\frac{\partial c_{b,i}}{\partial t} + \frac{(1-\varepsilon_b)3k_{1,i}}{\varepsilon_b R_p}\left(c_{b,i} - c_{p,i|r=R_p}\right) + r^{liq}_{kin,i} = D_{ax}\frac{\partial^2 c_{b,i}}{\partial x} + u\frac{\partial c_{b,i}}{\partial x}, \tag{14}$$

$$(1-\varepsilon_p)\frac{\partial q_i}{\partial t} + \varepsilon_p\frac{\partial c_{p,i}}{\partial t} - \varepsilon_p D_{p,i}\left[\frac{1}{r^2}\frac{\partial}{\partial r}\left(r^2\frac{\partial c_{p,i}}{\partial r}\right)\right] - r^{sol}_{kin,i} = 0, \tag{15}$$

where also reaction terms in the liquid and in the solid phase were included.

These two partial differential equations describe the concentrations in the mobile phase ($c_{b,i}$) and in the stationary phase (q_i and $c_{p,i}$). The adsorption isotherms relate the concentrations q_i (substance i adsorbed by the solid) and $c_{p,i}$ (substance i in the stationary liquid phase). A commonly utilized isotherm functional form is bi-Langmuir isotherm:

$$q_i = \frac{a_1 c_{p,i}}{1 + \sum_j b_{1j} c_{p,i}} + \frac{a_2 c_{p,i}}{1 + \sum_j b_{2j} c_{p,j}}. \tag{16}$$

An efficient numerical solution for the GRM incorporating arbitrary nonlinear isotherms was proposed by Gu (1995). The mobile phase and the stationary phase are discretized using the finite element and the orthogonal collocation method. The resulting ordinary differential equation (ODE) system is solved using an ODE solver which is based on the Gear's method for stiff ODEs. The numerical solution yields the concentrations of the components in the column at different locations and times. The concentration information at the outlet of the column is used to generate the chromatogram from which the production rate and the recovery yield can be computed.

The requirements on the products can usually be formulated in terms of minimum purities, minimum recoveries or maximum losses. In the case of a binary separation without intermediate cuts, these constraints can be transformed into each other, so either the recovery yield or the product purity may be constrained. The production cost is determined by many factors, in particular the throughput, the solvent consumption and the cost of downstream processing. A simple objective function is the productivity Pr, i.e., the amount of product produced per amount of adsorbent. This formulation results in the following nonlinear dynamic optimization problem:

$$\begin{aligned} \max \quad & \mathrm{Pr}(u, t_{cyc}, t_{inj}) = \frac{\dot{m}_{Product}}{m_{Adsorbent}} \\ \text{such that} \quad & \mathrm{Rec}_i \geq \mathrm{Rec}_{min,i}, \quad i = 1, \ldots, n_{sp} \\ & 0 \leq u \leq u_{max}, \\ & 0 \leq t_{inj}, t_{cyc} \end{aligned} \tag{17}$$

where Rec_i denotes the revovery yield of product i.

This type of problem can be solved by standard optimization algorithms. In order to reduce the computation times to enable online optimization, Dünnebier et al. (2001) simplified the optimization problem and decomposed it in order to enable a more

efficient solution. They exploited the fact that the recovery constraints are always active at the optimal solution and consider them as equalities. The resulting solution algorithm consists of two stages, the iterative solution of the recovery equality constraints, and the solution of the remaining unconstrained static nonlinear problem.

4.3.2 Model-based Control with Model Adaptation

In industrial practice, chromatographic separations are usually controlled manually. However, automatic feedback control leads to a uniform process operation closer to the economic optimum, and it can include online reoptimization. Dünnebier et al. (2001) proposed the model-based online optimization strategy shown in Figure 4.8.

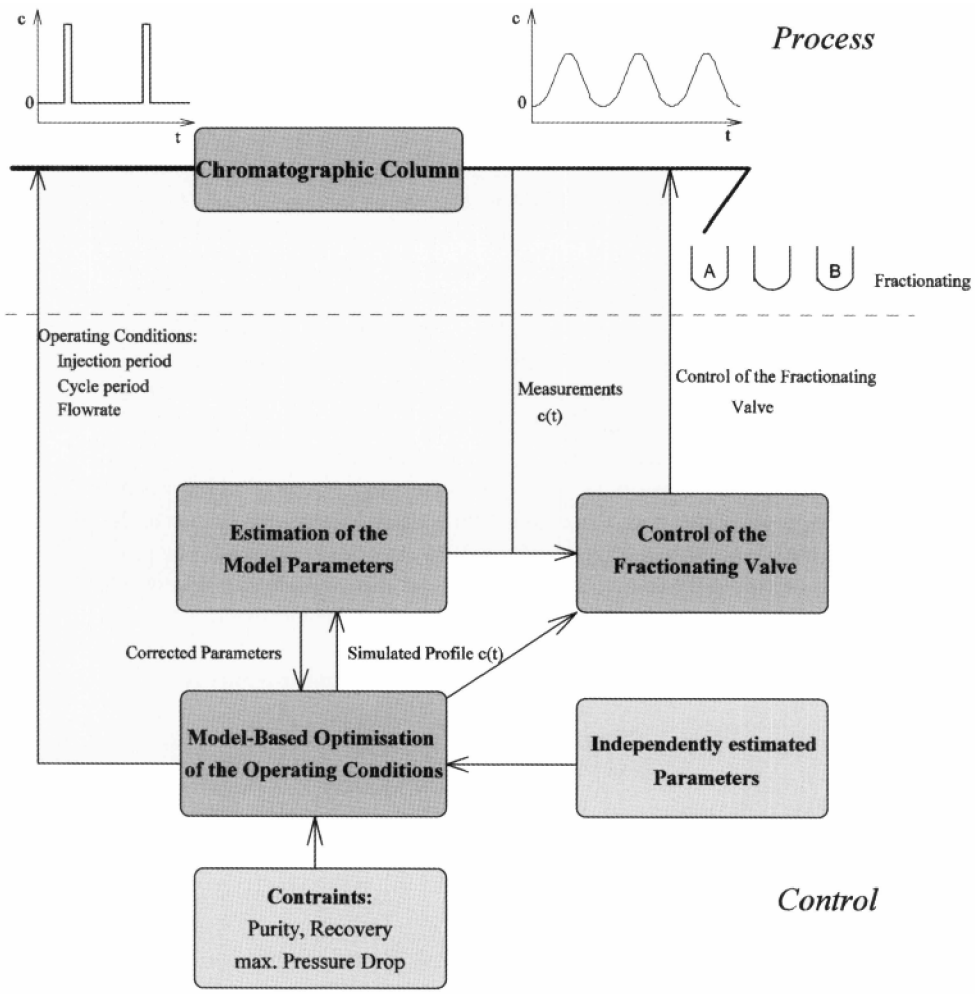

Figure 4.8 Control scheme for chromatographic batch separations

Essentially, this scheme performs the above optimization of the operating parameters online. To improve the model accuracy and to track changes in the plant, an online parameter estimation is performed. A similar run-to-run technique has been proposed by Nagrath et al. (2003).

Note that this scheme contains feedback only in the parameter estimation path. Therefore it will lead to good results only if the model is structurally correct so that the parameter estimation leads to a highly accurate model.

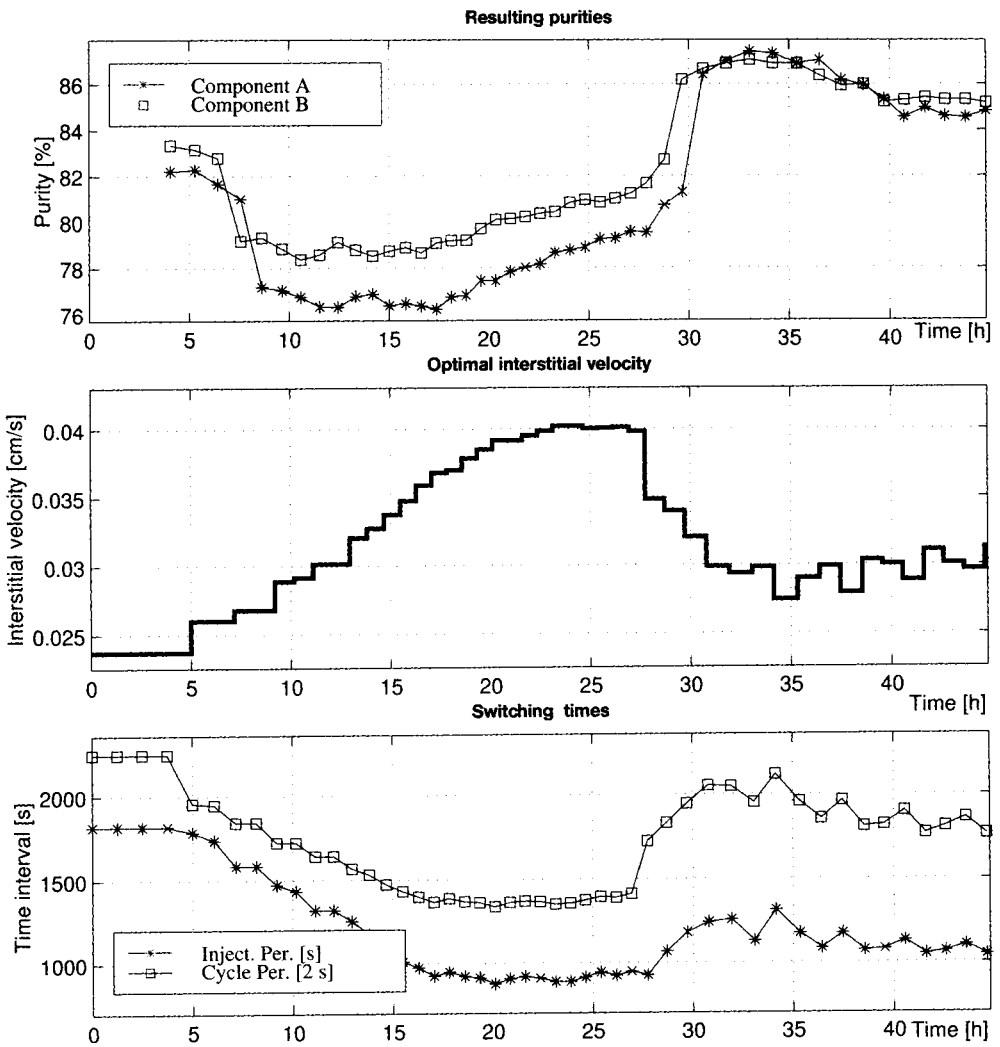

Figure 4.9 Product purities and operating parameters during an experimental run (set-point change for required purity at approximately 28 h from 80 to 85 %) (from Dünnebier et al., 2001)

The scheme was tested successfully at the pilot scale for a sugar separation with linear adsorption isotherm by Dünnebier et al. (2001). The product concentrations were measured using a two-detector concept as first proposed by Altenhöhner et al. (1997). A densimeter was used for the measurement of the total concentration of fructose and glucose and a polarimetric detector for the determination of the total rotation angle. Both devices were installed in series at the plant outlet.

Figure 4.9 shows an experimental result. First the operating parameters are modified in order to meet the product purity and recovery of 80 % each. After about 28 h, the controlled operating parameters reach a stable steady state. At this point a set-point change takes place in the product specifications: purity and recovery are now required to be 86 %. The control scheme reacts immediately, reducing the interstitial velocity and increasing the injection and cycle intervals. This leads to a better separation of the two peaks and to an increase in purity as desired. The controlled system quickly converges to a new steady state.

4.3.3 Summary

The key idea of the approach described in this section is to use model-based set-point optimization for model-based closed-loop control. Plant-model mismatch is tackled by adapting key model parameters to the available measurements so that the concentration profiles at the output which are predicted by the model match the observed ones. Experimental results showed that this approach works very well in the case of sugar separations where the model is structurally correct. The optimization algorithm was tailored to the structure of the problem so that convergence problems were avoided. Owing to the use of a tailored algorithm and the fact that the process is quite slow, computation times were not a problem.

4.4 Control by Measurement-based Online Optimization

In the two-step approach described in the previous section, the model parameters are updated by a parameter estimation procedure so that the model represents the plant at current operating conditions as accurately as possible. The updated model is used in the optimization procedure to generate a new set-point. This method works well for parametric mismatch between the model and the real plant. However, it does not guarantee an improvement of the set-point when structural errors in the model are present. In chromatographic separations, structural errors result e.g., from the approximation of the real isotherm by the Bi-Langmuir function. One important cause of plant-model mismatch can be the presence of small additional impurities in the mixture which may lead to considerable deviations of the observed concentration profiles at the output. The model-based optimization then generates a suboptimal operating point which in general does not satisfy the constraints on purity or recovery. The conventional solution is to introduce an additional control loop that regu-

lates the product purities, as proposed and tested by Hanisch (2002). However, the changes of the operating parameters caused by this control loop may conflict with the goal of optimizing performance.

4.4.1 The Principle of Iterative Optimization

To cope with structural plant-model mismatch, the available measurements can be used not only to update the model but also to modify the optimization problem in such a manner that the gradient of the (unknown) real process mapping is driven to zero, in contrast to satisfying the optimality conditions for the theoretical model. Such an iterative two-step method was proposed by Roberts (1979), termed integrated system optimization and parameter estimation (ISOPE). A gradient-modification term is added to the objective function of the optimization problem. ISOPE generates set-points which converge towards the true optimum despite parametric and structural model mismatch. Theoretical optimality and convergence of the method were proven by Brdyś et al. (1987). From a practical point of view, the key element of ISOPE is the estimation of the gradient of the plant outputs with respect to the optimization variables.

The general model-based set-point optimization problem can be stated as

$$\begin{aligned} \min_{\mathbf{u}} \quad & J(\mathbf{u}, \mathbf{j}) \\ \text{such that} \quad & \mathbf{g}(\mathbf{u}) \leq 0 \\ & \mathbf{u}_{\min} \leq \mathbf{u} \leq \mathbf{u}_{\max} \end{aligned} \tag{18}$$

where $J(\mathbf{u},\mathbf{y})$ is a scalar objective function, $\mathbf{u}$ is a vector of optimization variables (set-points), $\mathbf{y}$ is a vector of output variables, and $\mathbf{g}(\mathbf{u})$ is a vector of constraint functions. The relationship between $\mathbf{u}$ and $\mathbf{y}$ is represented by a model

$$\mathbf{y} = \mathbf{f}(\mathbf{u}, \alpha) \tag{19}$$

where α is a vector of model parameters. ISOPE is an iterative algorithm, where at each step of the iteration measurement information (i.e., the plant output $\mathbf{y}^*$, which was measured after the last set-point was applied) is used to update the model and to modify the optimization problem. The updating of the model can be realized as a parameter estimation procedure. A vector of gradient modifiers is computed using the gradient of the updated model and of the plant at set-point $\mathbf{u}^{(k)}$:

$$\lambda^{(k)} = \left((\mathbf{y}^*)'_{\mathbf{u}} - \mathbf{y}'_{\mathbf{u}}\right) J'_{\mathbf{y}}(\mathbf{u}, \mathbf{y})\Big|_{\mathbf{u}^{(k)}}. \tag{20}$$

The optimization problem of Eq. (18) is modified by adding a gradient-modification term to the objective function:

$$\begin{aligned} \min_{\mathbf{u}} \quad & J(\mathbf{u}, \mathbf{y}) + \lambda^{(k)^{\mathrm{T}}} \mathbf{u} \\ \text{such that} \quad & \mathbf{g}(\mathbf{u}) \leq 0 \\ & \mathbf{u}_{\min} \leq \mathbf{u} \leq \mathbf{u}_{\max}. \end{aligned} \tag{21}$$

Assuming that the constraint function $\mathbf{g}(\mathbf{u})$ is known, the optimization problem can be solved by any nonlinear optimization algorithm. Let $\hat{\mathbf{u}}^{(k)}$ denote the solution to Eq. (21), then the next set-point is chosen as:

$$\mathbf{u}^{(k+1)} = \mathbf{u}^{(k)} + \mathbf{K}\left[\hat{\mathbf{u}}^{(k)} - \mathbf{u}^{(k)}\right] \tag{22}$$

where $\mathbf{K}$ is a diagonal gain matrix, the diagonal elements are in the interval [0,1], i.e., $\mathbf{K}$ is a damping term. Starting from an initial set-point, ISOPE will generate a sequence of set-points which, for an appropriate gain matrix, will converge to a set-point which satisfies the necessary optimality conditions of the actual plant. It can be proven that the modification term leads to the satisfaction of the optimality conditions at the true plant optimum.

Tatjewski (2002) redesigned the ISOPE method resulting in a new algorithm that does not require the parameter estimation procedure. The key idea is to introduce a model shift term in the modified objective function:

$$\min_{\mathbf{u}} = J\left(\mathbf{u}, \mathbf{y} + \mathbf{a}^{(k)}\right) + \lambda^{(k)^T}\mathbf{u} \tag{23}$$

with the following definition of the modifier

$$\lambda^{(k)} = \left(\left(\mathbf{y}^*\right)'_{\mathbf{u}} - \mathbf{y}'_{\mathbf{u}}\right) J'_{\mathbf{y}}\left(\mathbf{u}, \mathbf{y} + \mathbf{a}^{(k)}\right)\Big|_{\mathbf{u}^{(k)}} \tag{24}$$

Here

$$\mathbf{a}^{(k)} = \mathbf{y}^{*(k)} - \mathbf{y}^{(k)}. \tag{25}$$

Although the parameter α is not updated, it is can be proven that the optimality conditions are satisfied. Parameter adaptation thus is no longer necessary, although it may be beneficial to the convergence of the procedure. As the optimality of the result is solely due to the gradient-modification in the optimization problem, the redesigned algorithm could be termed *iterative gradient-modification optimization.*

4.4.2
Handling of Constraints

If constraint functions depend on the behavior of the real plant, they cannot be assumed to be precisely known, and using a model for the computation of the constraint functions will not assure that the constraints are actually satisfied. In the original derivation of the ISOPE method, constraints were assumed to be process-independent. An extension of the ISOPE strategy which considers process-dependent constraints can be found in Brdyś et al. (1986). In this formulation, a recursive Lagrange multiplier is used. Tatjewski et al. (2001) also proposed using a follow-up constraint controller that is responsible for satisfying the output constraints.

A different method to handle the process-dependent constraints was proposed in Gao and Engell 2005. It is based on the idea of using plant information acquired at

the last set-point $\mathbf{g}^*(\mathbf{u}^{(k)})$ to modify the model-based constraint functions $\mathbf{g}(\mathbf{u})$ at the current iteration. The modified constraint functions approximate the true constraint functions of the plant in the vicinity of the last set-point. The modified constraint function is formulated as:

$$\hat{\mathbf{g}}^{(k)}(\mathbf{u}) = \mathbf{g}(\mathbf{u}) + \mathbf{g}^*(\mathbf{u}^{(k)}) - \mathbf{g}(\mathbf{u}^{(k)}) + \left((\mathbf{g}^*)'_{\mathbf{u}}(\mathbf{u}^{(k)}) - \mathbf{g}'_{\mathbf{u}}(\mathbf{u}^{(k)})\right)(\mathbf{u} - \mathbf{u}^{(k)}). \tag{26}$$

The modified constraint function has the following properties at $\mathbf{u}^{(k)}$:

- The modified constraint has the same value as the real constraint function, $\hat{\mathbf{g}}^{(k)}(\mathbf{u}^{(k)}) = \mathbf{g}^*(\mathbf{u}^{(k)})$.
- The modified constraint has the same first order derivative as the real constraint function, $(\hat{\mathbf{g}}^{(k)})'_{\mathbf{u}}(\mathbf{u}^{(k)}) = (\mathbf{g}^*)'_{\mathbf{u}}(\mathbf{u}^{(k)})$.

As the modified constraint is only valid in the vicinity of $\mathbf{u}^{(k)}$, a bound $\mathbf{u}^{(k)} - \Delta\mathbf{u} \leq \mathbf{u} \leq \mathbf{u}^{(k)} + \Delta\mathbf{u}$ is added to the optimization problem to limit the search range in the next iteration. This guarantees that the constraints are not violated greatly.

4.4.3
Estimation of the Gradient of the Plant Mapping

A key element of the iterative gradient-modification optimization method is to estimate the gradient of the plant mapping. Several methods for this have been proposed during the last 20 years. These methods can be grouped into two categories according to whether set-point perturbations are used or not. Early versions of the ISOPE technique used finite difference techniques to obtain the plant gradient by applying perturbations to the current set-point. Later versions used dynamic perturbations and linear system identification methods to estimate the gradient (Lin et al. 1989, Zhang and Roberts 1990). Both methods have the disadvantage of requiring additional perturbations. In Roberts (2000), Broyden's formula was used to estimate the required gradient from current and past measurement information. The Broyden estimate is updated at each iteration using a formula of the form:

$$D^{(k)} = D^{(k-1)} + \frac{\left[\Delta Y^{(k)} - D^{(k-1)}\Delta X^{(k)}\right]\left(\Delta X^{(k)}\right)^{\mathrm{T}}}{\left(\Delta X^{(k)}\right)^{\mathrm{T}}\Delta X^{(k)}} \tag{27}$$

with

$$\Delta Y^{(k)} = Y^{(k)} - Y^{(k-1)}$$
$$\Delta X^{(k)} = X^{(k)} - X^{(k-1)}$$

where D is the estimate of $\partial Y(X)/\partial X$, and the superscript k refers to the iteration index. Although no additional perturbation is needed, care must be taken to avoid ill-conditioning as $\Delta X^{(k)} \rightarrow 0$. It should also be noted that the updating formula requires to be initialized with $D^{(0)}$. Brdyś and Tajewski (1994) proposed a different way of implementing a finite difference approximation of the gradient without additional set-point perturbations. This method uses set-points in past iterations instead

of additional set-point perturbations. The gradient at set-point $\mathbf{u}^{(k)}$ is approximated as:

$$\left(\mathbf{y}^*\right)'_{\mathbf{u}}\Big|_{\mathbf{u}^{(k)}} \approx \left(\mathbf{S}^{(k)}\right)^{-1} \cdot \begin{bmatrix} \mathbf{y}^{*(k)} - \mathbf{y}^{*(k-1)} \\ \vdots \\ \mathbf{y}^{*(k)} - \mathbf{y}^{*(k-m)} \end{bmatrix} \tag{28}$$

with

$$\mathbf{S}^{(k)} = \left[\mathbf{u}^{(k)} - \mathbf{u}^{(k-1)}, \ldots, \mathbf{u}^{(k)} - \mathbf{u}^{(k-m)}\right]^{\mathrm{T}}$$

where m is the dimension of the vector $\mathbf{u}$. Theoretically, the smaller the difference between the set-points, the more accurate will the approximation of the gradient be. On the other hand, because the measurements of the plant outputs $\mathbf{y}^{*(k-i)}$, $i = 0,1,\ldots,$ m are usually corrupted by errors, the matrix $\mathbf{S}^{(k)}$ should be sufficiently well-conditioned to obtain a good approximation of the gradient. Let

$$d^{(k)} = \frac{\sigma_{\min}\left(\mathbf{S}^{(k)}\right)}{\sigma_{\max}\left(\mathbf{S}^{(k)}\right)} \tag{29}$$

denote the conditioning of $\mathbf{S}^{(k)}$ in terms of its singular values. If $d^{(k)}$ is too small, the errors in the measurements will be amplified considerably and the gradient estimation will be corrupted by noise. In Brdyś and Tajewski (1994) the optimization problem is reformulated to take into account future requirements of the gradient estimation. An inequality constraint

$$d^{(k)} \geq \delta \tag{30}$$

(where $0 < \delta < 1$) is added to the optimization problem at the $(k-1)^{\text{th}}$ iteration so that the set-point $\mathbf{u}^{(k)}$ will give a good approximation of the gradient. The advantage of this method is that no additional set-point perturbations are needed, but a loss of optimality will be observed at the current iteration because the inequality constraint reduces the feasible set of set-points. Therefore more iterations are required to attain the optimum, especially for a bigger values of δ.

A novel method was proposed for the gradient estimation in Gao and Engell (2005). It follows the same idea as Brdyś's method, i.e., using the past set-points in the finite difference approximation of the gradient. But the conditioning of $\mathbf{S}^{(k)}$ is included not as a constraint in the optimization problem, but as an indicator to decide whether an additional set-point perturbation should be added. At the $(k-1)^{\text{th}}$ iteration, after a new set-point $\mathbf{u}^{(k)}$ is acquired, $d^{(k)}$ is computed using $\{\mathbf{u}^{(k)}, \mathbf{u}^{(k-1)}, \ldots, \mathbf{u}^{(k-m)}\}$. If it is less than the given constant δ, an additional set-point $\mathbf{u}_a^{(k)}$ will be added to formulate a new set-point set $\{\mathbf{u}^{(k)}, \mathbf{u}_a^{(k)}, \mathbf{u}^{(k-1)}, \ldots, \mathbf{u}^{(k-m-1)}\}$ for the gradient approximation. The gradient at $\mathbf{u}^{(k)}$ is approximated by:

$$\left(\mathbf{y}^*\right)'_{\mathbf{u}}\Big|_{\mathbf{u}^{(k)}} \approx \left(\mathbf{S}_a^{(k)}\right)^{-1} \cdot \begin{bmatrix} \mathbf{y}^{*(k)} - \mathbf{y}_a^{*(k)} \\ \mathbf{y}^{*(k)} - \mathbf{y}^{*(k-1)} \\ \vdots \\ \mathbf{y}^{*(k)} - \mathbf{y}^{*(k-m-1)} \end{bmatrix} \tag{31}$$

with

$$\mathbf{S}_a^{(k)} = \left[\mathbf{u}^{(k)} - \mathbf{u}_a^{(k)},\ \mathbf{u}^{(k)} - \mathbf{u}^{(k-1)}, \ldots, \mathbf{u}^{(k)} - \mathbf{u}^{(k-m-1)}\right]^T.$$

The additional set-point provides an additional perturbation around the current set-point. Its location is optimized by solving

$$\begin{aligned} \max_{\mathbf{u}_a^{(k)}} \quad & d_a^{(k)} = \frac{\sigma_{\min}\left(\mathbf{S}_a^{(k)}\right)}{\sigma_{\max}\left(\mathbf{S}_a^{(k)}\right)} \\ \text{such that} \quad & \hat{\mathbf{g}}^{(k-1)}\left(\mathbf{u}_a^{(k)}\right) \le 0 \\ & \mathbf{u}^{(k-1)} - \Delta\mathbf{u} \le \mathbf{u}_a^{(k)} \le \mathbf{u}^{(k-1)} + \Delta\mathbf{u} \\ & \mathbf{u}_{\min} \le \mathbf{u}_a^{(k)} \le \mathbf{u}_{\max}. \end{aligned} \tag{32}$$

Therefore, by introducing the additional set-point, $\mathbf{S}_a^{(k)}$ is kept well-conditioned and the optimal set-point $\mathbf{u}^{(k)}$ can be used in the gradient approximation. This method does not compromise optimality, and it is not as expensive as finite difference techniques with set-point perturbations in each iteration, because an additional set-point perturbation is added only when $d^{(k)} < d$.

The procedure can be summarized as follows:

1. Select starting set-points which include the initial set-point and m other set-points for the gradient estimation at the initial set-point. Initialize the parameters of the algorithm, i.e., K, δ and $\Delta\mathbf{u}$.
2. At the k^{th} iteration, apply set-point $\mathbf{u}^{(k)}$ (and $\mathbf{u}_a^{(k)}$ if needed) to the plant. Measure the steady-state outputs.
3. Approximate the gradient using the proposed method. Modify the objective function and the constraint functions in the optimization problem and add the additional bound.
4. Solve the modified optimization problem Eqs. (23)–(26) using any nonlinear optimization algorithm and generate the next set-point.
5. Check the termination criterion $\|\mathbf{u}^{(k+1)} - \mathbf{u}^{(k)}\| < \varepsilon$ and decide whether to continue or to stop the optimization procedure.
6. If the termination criterion is not satisfied, check the conditioning of $\mathbf{S}^{(k)}$ in terms of its singular values

$$d^{(k)} = \frac{\sigma_{\min}\left(\mathbf{S}^{(k)}\right)}{\sigma_{\max}\left(\mathbf{S}^{(k)}\right)},$$

   and if $d^{(k)} \ge \delta$ return to step 2, otherwise go to step 7.
7. Add an additional set-point by solving the optimization problem Eq. (32), then return to step 2.

4.4.4 Application to a Batch Chromatographic Separation with Nonlinear Isotherm

The iterative gradient-modification optimization method was tested in a simulation study of a batch chromatographic separation of enantiomers with highly nonlinear adsorption isotherms that had been used as a test case in laboratory experiments before (Hanisch 2002). A model with a bi-Langmuir isotherm that was fitted to measurement data is considered as the "real plant" in the simulation study. A model with isotherms of a different form is used in the set-point optimization.

The flow rate Q and the injection period t_{inj} are considered as the manipulated variables here. The cycle period t_{cyc} is fixed to the duration of the chromatogram. The performance criterion is the production rate Pr:

$$\mathrm{Pr} = m_{\mathrm{product}}/t_{\mathrm{cyc}} \tag{33}$$

The recovery yield Rec is constrained to a minimal value. This results in the optimization problem

$$\begin{aligned} \max_{Q,t_{\mathrm{inj}}} \quad & \mathrm{Pr}(Q, t_{\mathrm{inj}}) \\ \text{such that} \quad & \mathrm{Rec}(Q, t_{\mathrm{inj}}) \geq \mathrm{Rec}_{\min} \\ & 0 \leq Q \leq Q_{\max} \\ & t_{\mathrm{inj}} \geq 0 \end{aligned} \tag{34}$$

Figure 4.10 shows the chromatograms of the "real" and the perturbed model for the same set-point. Note that such differences can be generated by rather small errors in the adsorption isotherms.

The second component is considered to be the valuable product. The purity requirement is 98%. The recovery yield should be greater than 80%. There is an upper limit of the flow rate of 2.06 $\mathrm{cm^3\,s^{-1}}$. The flow rate and the injection period are normalized to the interval [0, 1] in the optimization. The gain coefficients in $\mathbf{K}$ are set to 1. The bound $\Delta\mathbf{u}$ is $[.06\ .06]^T$. The recovery constraint was handled by the method

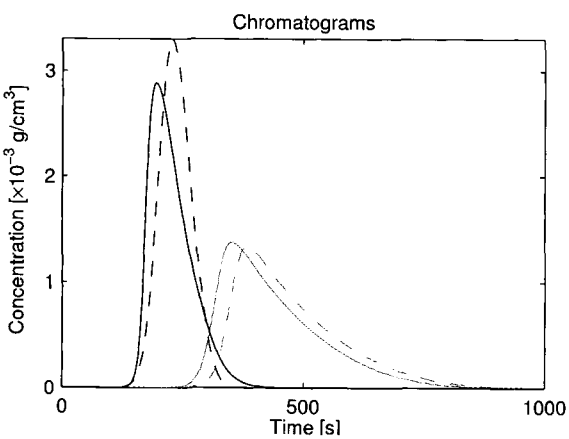

Figure 4.10 Illustration of the influence of model mismatch on the chromatogram. *Solid line*: "real" model; *dashed line*: nominal optimization model

proposed above. The iterations were stopped when the calculated set-point change was less than a predefined tolerance value ($\varepsilon = 0.006$) or the optimization algorithm did not terminate successfully.

Different gradient estimation methods were used in the iterative optimization procedure:

- the finite difference method, i.e., applying perturbations to each set-point (FDP);
- Brdyś's method, where an additional constraint is added to the optimization problem so that the next set-point can be used in the estimation of the gradient, no perturbations;
- finite difference method with additional set-point perturbations when necessary (FDPN).

Several runs of the set-point optimization were simulated, first without measurement errors and then with errors. In the case without errors, the optimization procedures with FDP and FDPN terminated successfully, while the optimization procedure with Brdyś's method stopped early because the optimization algorithm could not find a feasible point in the given number of iterations. The optimization procedure with FDPN used one iteration more than the optimization procedure with FDP, but it used only six additional set-points ($\delta = 0.2$). The optimization procedure with FDP perturbed the set-point eight times at each iteration to estimate the gradient so that it generated 80 additional set-points overall. The trajectories of the production rate Pr and of the recovery yield Rec are depicted in Figure 4.11. The recovery constraint was met by all three optimization procedures. Figure 4.12 shows the set-point trajectories and the production rate and recovery contours of the real model and the optimization model. Although a considerable mismatch exists between the real model and the optimization model, the iterative gradient-modification optimization method generates set-points which converge to the real optimum.

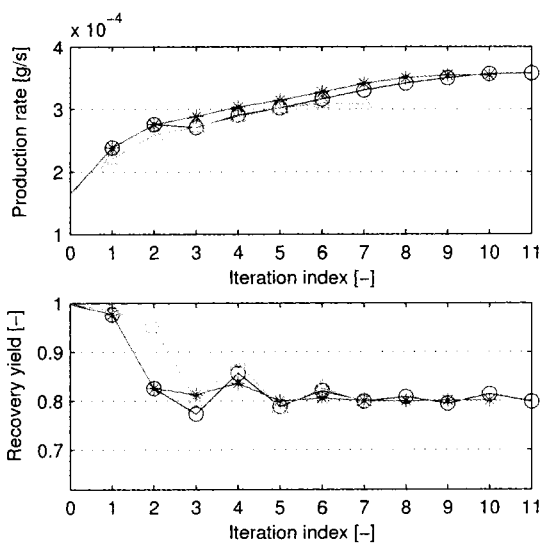

Figure 4.11 Trajectories of production rate and recovery yield, simulations without errors. * Set-points using the finite difference method (FDP), Δ set-points using Brdyś's method, o set-points using the finite difference method with additional set-point perturbations when necessary (FDPN). Recovery limit: 80 %, $\delta = 0.2$

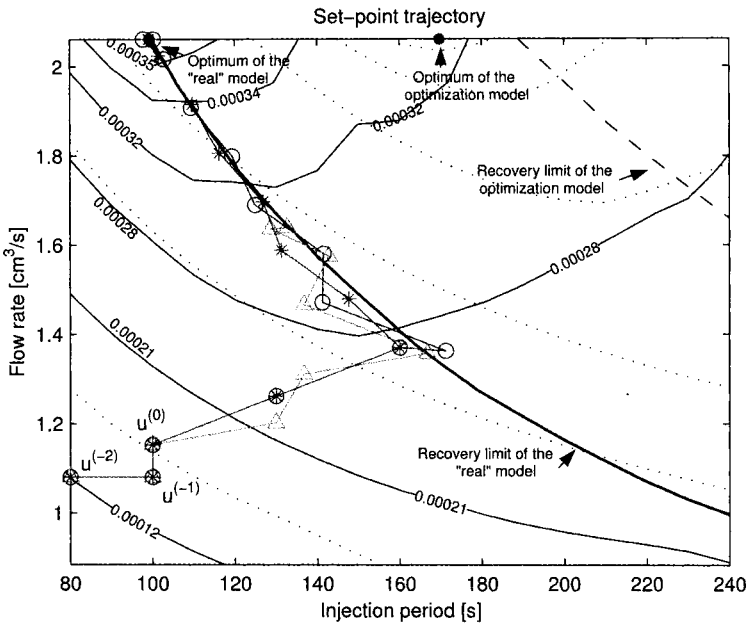

Figure 4.12 Illustration of set-point trajectories. *Solid lines*: contours of the "real" model; *dotted lines*: contours of the nominal optimization model, * set-points using FDP method, Δ set-points using Brdyś's method, *o* set-points using FDPN method, $u^{(0)}$ initial set-point, $u^{(1)}$ and $u^{(2)}$ additional initial set-points for the gradient estimation at $u^{(0)}$

Table 4.1 shows the results of simulations with measurement errors. Different values of δ were tried and all simulations were stopped at the optimum of the "real" model. With increasing δ, more additional set-points were used, which improved the accuracy of the gradient estimations. Therefore, fewer iterations were needed to arrive at the optimum. Considering the total number of set-points used, $\delta = 0.1$ gives a good result.

Table 4.1 Optimization results of the simulations with errors

δ	Number of iterations	Additional set-points	Final set-point	Optimum of the "real" model
0.2	13	7	(2.06, 99.73).	(2.06, 99.35).
0.1	13	6	(2.06, 99.79).	
0.05	15	5	(2.06, 99.53).	
0.01	22	4	(2.06, 99.10).	

4.4.5 Summary

The identification of an accurate model requires considerable efforts, especially for chemical and biochemical processes. In practice, inaccurate models must be used for online control and optimization. A purely model-based optimization will generate a

suboptimal or even infeasible set-point. We described a modified iterative gradient-modification optimization strategy that converges to the real optimum in a few steps while respecting the constraints. A few additional set-points are introduced to reduce the effect of measurement errors on the gradient approximation. The example of a batch chromatographic separation with highly nonlinear isotherms demonstrated the impressive improvements that can be obtained by this approach.

4.5
Nonlinear Model-based Control of a Reactive Simulated Moving Bed (SMB) Process

4.5.1
Principle and Optimization of Chromatographic SMB Separations

Batch chromatography has the usual drawbacks of a batch operation, and leads to highly diluted products. On the other hand, it is extremely flexible, several components may be recovered from a mixture during one operation and varying compositions of the desorbent can be used to enhance separation efficiency. The idea of a continuous operation with countercurrent movement of the solid led to the development of the simulated moving bed (SMB) process (Broughton 1966). It is gaining increasing attention due to its advantages in terms of productivity and eluent consumption (Guest 1997, Juza et al. 2000). A simplified description of the process is given in Figure 4.13. It consists of several chromatographic columns connected in series which constitute a closed loop. A countercurrent motion of the solid phase relative to the liquid phase is simulated by periodically and simultaneously moving the inlet and outlet lines by one column in the direction of the liquid flow.

After a start-up phase, SMB processes reach a cyclic steady state (CSS). Figure 4.13 shows the CSS of a binary separation along the columns plotted for a fixed time instant within a switching period. At every axial position, the concentrations vary as

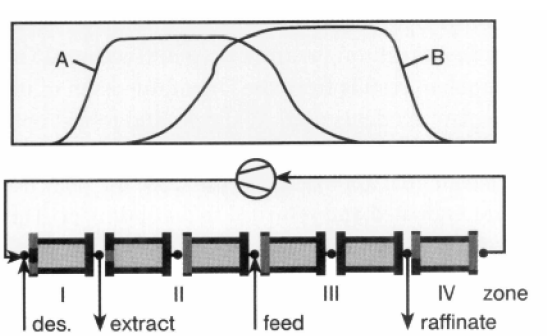

Figure 4.13 Simulated Moving-Bed Process. At the top, the concentration profiles at the cyclic steady state are shown. Pure a is withdrawn at the extract port and pure B is withdrawn at the raffinate port

a function of time, and the values reached at the end of each switching period are equal to those before the switching, relative to the port positions.

In order to exploit the full potential of SMB processes, recent research has focused on the design of the process, in particular the choice of the operation parameters for a given selection of adsorbent, solvent and column dimensions, using mathematical optimization. As the optimum should be determined precisely while meeting all constraints, rigorous models which include the discrete dynamics are used (Klatt et al. 2000, Zhang et al. 2003). In addition to a higher reliability compared to shortcut methods, this approach is applicable to a broad variety of SMB-like operating regimes. The optimization problem can be stated as (Toumi et al. 2004c):

$$\begin{aligned} \min_{Q_j, N_i, \tau} \quad & \mathrm{Cost}_{\mathrm{spec}} \\ \text{such that} \quad & \Gamma\left(\mathbf{c}_{\mathrm{ax}}(0)\right) - \mathbf{c}_{\mathrm{ax}}(\tau) \leq \varepsilon, \\ & \mathrm{Pur}_{\mathrm{Ex}} \geq \mathrm{Pur}_{\mathrm{Ex,min}}, \\ & \mathrm{Pur}_{\mathrm{Raf}} \geq \mathrm{Pur}_{\mathrm{Raf,min}}, \\ & 0 \leq Q_j \leq Q_{\max}, \end{aligned} \tag{35}$$

where $\mathrm{Pur}_{\mathrm{EX}}$ and $\mathrm{Pur}_{\mathrm{Raf}}$ denote the purities at the extract and the raffinate ports and Γ summarizes of dynamics of the process from one switching period to the next, including the shifting of the ports and c_{ax} denotes the axial concentration profile along the columns.

The goal is to operate the process at the optimal CSS with minimal separation costs $\mathrm{Cost}_{\mathrm{spec}}$ while the purity requirements at both product outlets are fulfilled. Equation (34) constitutes a complex dynamic optimization problem the solution of which critically depends on an efficient and reliable computation of the CSS defined by

$$\Gamma\left(\mathbf{c}_{\mathrm{ax}}(0)\right) - \mathbf{c}_{\mathrm{ax}}(\tau) \leq \varepsilon, \tag{36}$$

The free optimization variables are the flow rates in the sections Q_j and the switching period τ. They are transformed to the so-called β-factors, which represent the ratio between the flow rates Q_j and the hypothetical solid flow rate. This nonlinear transformation leads to a better conditioned optimization problem (Dünnebier et al. 2001). An additional constraint takes the maximum pressure drop into account. The main difficulty of the optimization problem results from the large dimension of the CSS equations when a first-principle plant model is used. A simple and robust optimization approach consists of integration of the model equations starting from initial values until the CSS is reached (sequential approach). At the CSS, the objective function as well as the constraints are evaluated and returned to an optimizer. This yields a small number of free parameters and hence a relatively simple optimization problem. The number of cycles required to reach a CSS usually is not too large (about 100) in contrast to other periodic processes like pressure swing adsorption where 1000 or more periods have to be simulated. The computational effort is therefore reasonable.

4.5.2 Model-based Control

Klatt et al. (2002) proposed a two-layer control architecture similar to the one used for batch chromatography, where the optimal operating trajectory is calculated at a low sampling rate by dynamic optimization based on a rigorous process model. The model parameters are adapted based on online measurements. The low-level control task is to keep the process on the optimal trajectory despite disturbances and plant/model mismatch. The controller is based on identified models gained from simulation data of the rigorous process model along the optimal trajectory. For the linear adsorption isotherm case, linear models are sufficient (Klatt et al. 2002), whereas in the nonlinear case neural networks (NN) were applied successfully (Wang et al. 2003). A disadvantage of this two-layer concept is that the stabilized front positions do not guarantee the product purities if plant-model mismatch occurs. Thus an additional purity controller is required.

Toumi and Engell (2004a) recently presented a nonlinear model-predictive control scheme and applied it to a three-zones reactive SMB (RSMB) process for glucose isomerization (Toumi and Engell 2004b, 2005). The key feature of this approach is that the production cost is minimized online, while the product purities are considered as constraints, thus real online optimization is performed, not trajectory tracking.

The following optimal control problem is formulated over the finite control horizon H_r:

$$
\begin{aligned}
&\min_{[\boldsymbol{\beta}_k,\ldots,\boldsymbol{\beta}_{k+H_r}]} \quad \Omega = \sum_{j=k}^{k+H_p} \left(\mathrm{Cost}(j) + \Delta\boldsymbol{\beta}_j^{\mathrm{T}}\mathbf{R}_j\Delta\boldsymbol{\beta}_j\right)\\
&\text{such that} \quad \begin{cases}\dot{\mathbf{x}}_j = f\left(\mathbf{x}_j, \boldsymbol{\beta}_j\right)\\ \mathbf{x}_{j+1,0} = \mathbf{P}\mathbf{x}_j\left(\tau(j)\right)\end{cases},\\
&\qquad \mathrm{Pur}_{\mathrm{Ex},H_r} + \Delta\mathrm{Pur}_{\mathrm{Ex}} \geq \mathrm{Pur}_{\mathrm{Ex,min}},\\
&\qquad \mathrm{Pur}_{\mathrm{Ex},H_p} + \Delta\mathrm{Pur}_{\mathrm{Ex}} \geq \mathrm{Pur}_{\mathrm{Ex,min}},\\
&\qquad \mathbf{g}(\boldsymbol{\beta}_j) \geq 0,\\
&\qquad 0 \leq Q_{I,j} \leq Q_{\max}, \quad j = k,\ldots,k+H_p.
\end{aligned}
\tag{37}
$$

The prediction horizon is discretized in cycles, where a cycle is a switching time τ(k) multiplied by the total number of columns. Equation (37) constitutes a dynamic optimization problem with the transient behavior of the process as a constraint. The objective function Ω is the sum of costs incurred for each cycle (e.g., desorbent consumption) and a regularizing term added in order to smooth the input sequence in order to avoid high fluctuations in the input sequence from cycle to cycle. The first equality constraint represents the plant model evaluated over the finite prediction horizon H_p. The switching dynamics are introduced via the permutation matrix **P**. Since the maximal attainable pressure drop by the pumps must not be exceeded, constraints are imposed on the flow rates in zone I. Further inequality constraints $\mathbf{g}(\boldsymbol{\beta}_j)$ are added in order to avoid negative flow rates during the optimization.

The control objective is reflected by the purity constraint over the control horizon H_r which is corrected by a bias term $\Delta \mathrm{Pur}_{\mathrm{Ex}}$ resulting from the difference between the last simulated and the last measured process output to compensate unmodeled effects:

$$\Delta \mathrm{Pur}_{\mathrm{Ex},k} = \mathrm{Pur}_{\mathrm{Ex},(k-1)} - \mathrm{Pur}_{\mathrm{Ex},k,\mathrm{meas}}. \tag{38}$$

A second purity constraint over the whole prediction horizon acts similar to a terminal constraint forcing the process to converge towards the optimal CSS. It should be pointed out that the control goal (i.e., to fulfil the extract purity) is introduced as a constraint. A feasible path SQP algorithm is used for the optimization (Zhou et al. 1997) which generates a feasible point before it starts to minimize the objective function.

4.5.3
Online Parameter Adaptation

The concentration profiles in the recycling line are measured and collected during a cycle. Since this measurement point is fixed in the closed-loop arrangement, the sampled signal includes information of all zones. During the start-up phase, an online estimation of the actual model parameters is started in every cycle. The quadratic cost functional $J_{\mathrm{est}}(\mathbf{p})$:

$$J_{\mathrm{est}} = \sum_{i=1}^{n_{\mathrm{sp}}} \left(\int_0^{N_{\mathrm{col}}} \left(c_{i,\mathrm{meas}}(t) - c_{i,\mathrm{Re}}(t) \right)^2 \right) \tag{39}$$

is minimized with respect to the parameters p. For this purpose, the least squares solver E04UNF from the NAG-library is used. A by-product of the parameter estimation is the actual value $\mathbf{x}_0(k)$ of the state vector which is given back to the NMPC controller.

4.5.4
Simulation Study

Figure 4.14 shows a simulation scenario where the desired extract purity was set to 70 % at the beginning of the experiment. The desired extract purity was then changed to 60 % at cycle 60. At cycle 120, the desired extract purity was increased to 65 %. The enzyme activity and nonce the reaction rate is assumed to decay exponentially during the experiment. A fast response of the controller in both directions can be observed. Compared to the uncontrolled case, the controller can control the product purity and compensate the drift in the enzyme activity. The evolution of the optimizer iterations is plotted as a dashed line and shows that a feasible solution is found rapidly and that the concept can be realized in real time. In this example, the control horizon was set to two cycles and the prediction horizon to ten cycles. A diagonal matrix $\mathbf{R}_j = 0.02\ \mathbf{I}_{(3,3)}$ was chosen for regularization.

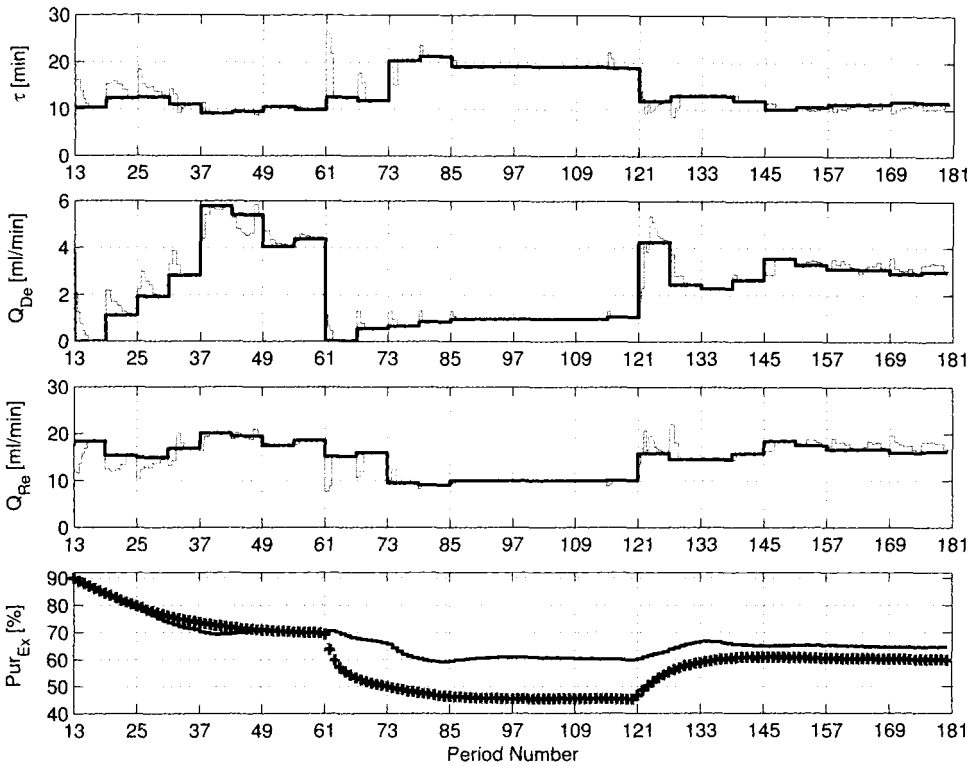

Figure 4.14 Control scenario $H_r = 2$, $H_p = 10$

Figure 4.15 shows the result of the parameter estimation. A good fit was achieved and the estimated parameter follows the drift of the reaction rate adequately.

4.5.5 Experimental Study

A sensitivity analysis showed that the process is highly sensitive to the values of the Henry coefficients, the mass transfer resistances and the reaction rate. These are therefore key parameters of the reactive SMB process. These parameters are reestimated online at every cycle (a cycle is equal to switching time multiplied by the number of columns). In Figure 4.16, the concentration profiles collected in the recycling line are compared to the simulated ones. At the end of the experiment all system parameters have converged towards stationary values as shown by Figure 4.17. The developed mathematical model describes the behavior of the RSMB process well.

The formulation of the optimization problem (37) was slightly modified for the experimental investigation. The sampling time of the controller was reduced to one switching period instead of one cycle, so that the controller reacts faster. The switching time was still used as a controlled variable, but modified only from cycle to

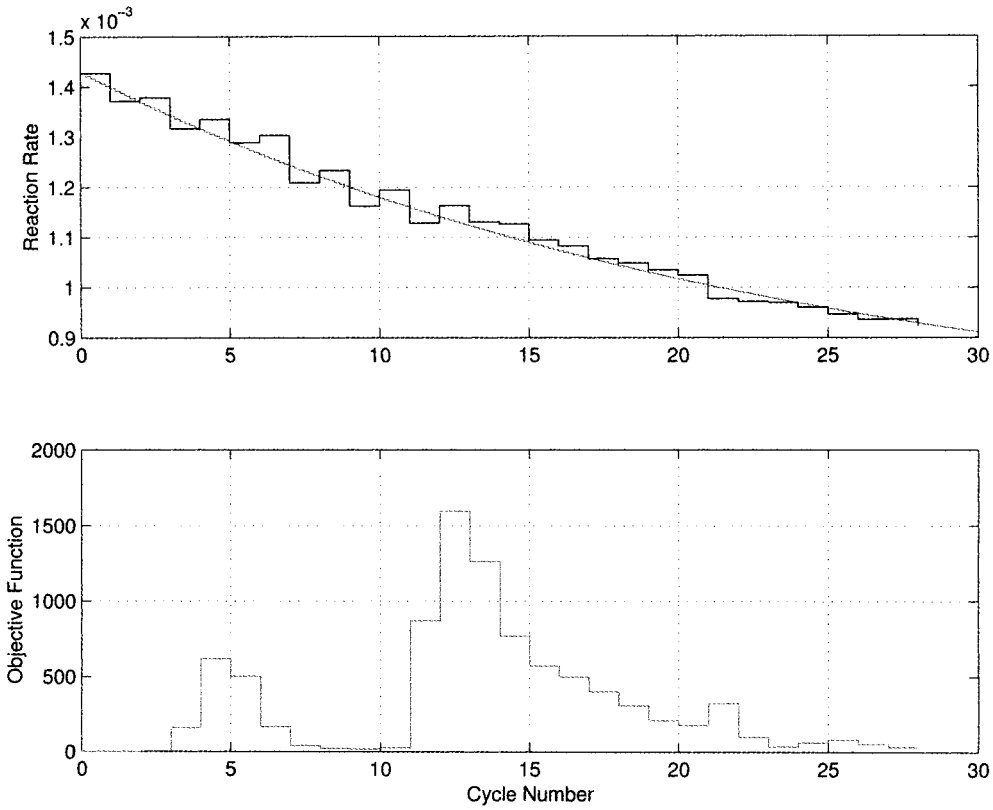

Figure 4.15 Estimation of the reaction rate

cycle. This is due to the asymmetry of the RSMB process that results from the dead volume of the recycling pump in the closed loop. It disturbs the overall performance of the process and is corrected by adding a delay for the switching of the inlet/outlet line passing the recycling pump. A detailed description of this method is provided in the patent (Hotier 1996). Therefore the shift of the valves is not synchronous to compensate for the technical imperfection of the real system and to get closer to the ideal symmetrical SMB system. In order to avoid port overlapping, the switching time must be held constant during a cycle.

In the real process, the enzyme concentration changes from column to column. The geometrical lengths of the columns also differ slightly. Moreover, the temperature is not constant over the columns due to the inevitable gradient of the closed heating-circuit. These problems cause a fluctuation of the concentration profiles at the product outlet. Even at the CSS, the product purity changes from period to period. Using the bias term given by Eq. (38) causes large variations of the controlled inputs from period to period. This effect was damped by using the minimal value over the last cycle:

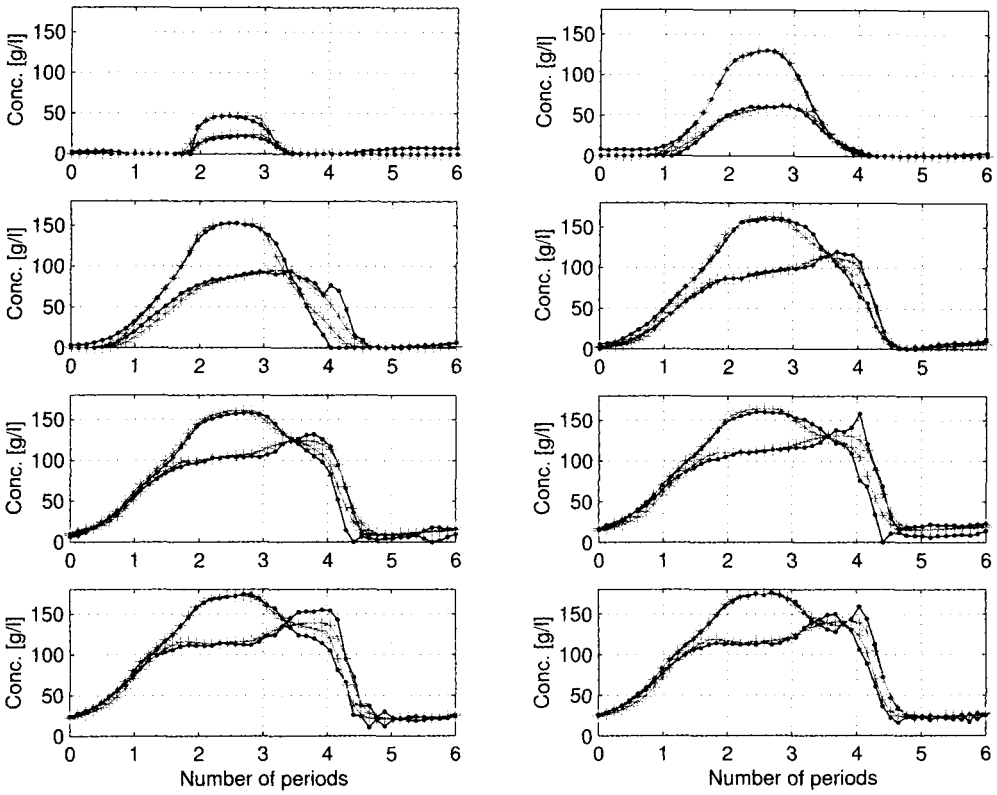

Figure 4.16 Comparison of experimental and simulated concentration profiles collected at the recycle line

$$\Delta \mathrm{Pur}_{\mathrm{Ex},k} = \min_{j=(k-1,\ldots,k-1-N_{\mathrm{col}})} \left(\mathrm{Pur}_{\mathrm{Ex},(k-1)} - \mathrm{Pur}_{\mathrm{Ex},k,\mathrm{meas}}\right), \tag{40}$$

The desired). purity for the experiment reported below was 55.0 % and the controller was started at the 60$^{\mathrm{th}}$ period. As in the simulation study, a diagonal matrix $\mathbf{R}_j = 0.02\,\mathbf{I}_{(3,3)}$ was chosen for regularization. The control horizon was set to $H_r = 1$ and the prediction horizon is H_p=60 periods. Figure 4.18 shows the evolution of the product purity as well as of the controlled variables. In the open-loop mode where the operating point was calculated based on the initial model, the product purity was violated at the periods numbered 48 and 54. After a cycle the controller was able to drive the purity above 55.0% and to keep it there. The controller first reduces the desorbent consumption. This action seems to be in contradiction to the intuitive idea that more desorbent injection should enhance the separation. In the presence of a reaction this is not true, as shown by this experiment. The controlled variables converge towards a steady state, but they still change from period to period, due to the nonideality of the plant.

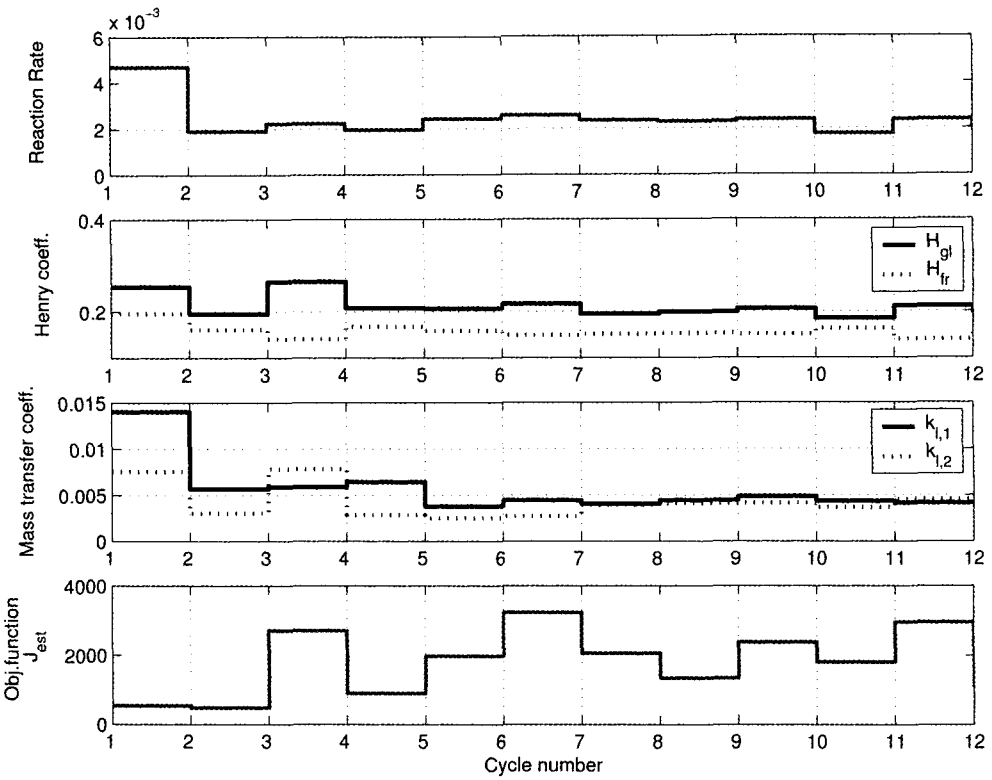

Figure 4.17 Online estimation of the model parameters

4.5.6 Summary

Closed-loop control of SMB processes is a challenging task because of the complex dynamics of the process and the large order of the discretized model. By formulating the control task as an online optimization problem on a receding horizon, the process can be at an optimal operating point while meeting constraints on the product purities. The feasibility of the approach has been demonstrated on a real pilot-scale plant using an industrial PLC-based in a well-known term.

4.6 Conclusions

In this chapter, it was demonstrated by means of several examples how rigorous, first-principles-based models can be used in process control. In the reactive distillation case study, a NMPC was presented that is based upon a slightly simplified rigorous process model. For reasons of computational efficiency, the solution of the algebraic equations was separated from the solution of the balance equations, resulting

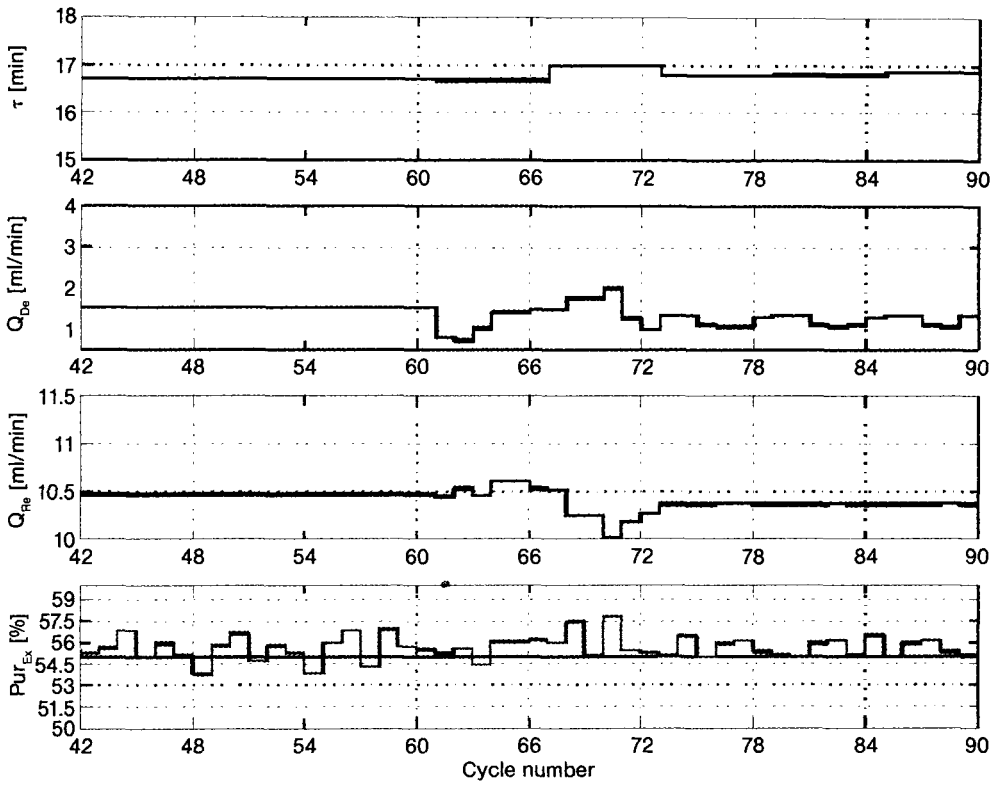

Figure 4.18 Control experiment for a target purity of 55.0 %

in a performance gain by about 10. The NMPC controller not only gave a much better performance than the linear controller but it could also control the process in a region where the gains change their signs so that a linear controller inevitably fails. In related work, we used a neural net approximation of the rigorous process model in an NMPC controller, giving a slightly inferior performance with a much reduced computational effort (Engell and Fernholz 2003).

Online optimization using measurement information in many cases is an attractive alternative to the tracking of precomputed references because the process can be operated much closer to its real optimum, while still meeting hard bounds on the specifications. The measurement information can be used in the control scheme in various ways. The weakest form of feedback is to use the measurements for parameter adaptation only which requires a structurally correct model. In the control of the SMB process, this was combined with updating a disturbance model so that the desired product purities were maintained even for plant-model mismatch. Measurement information can also be used to modify the gradients in the optimization problem, ensuring convergence to the true optimum even in the case of structural model mismatch.

The biggest obstacle to the widespread use of model-based control is the effort needed to obtain faithful dynamic models of complex processes. While it has become

routine to base process design on rigorous stationary process models, the effort to develop dynamic models is usually avoided. Process designers tend to neglect dynamic effects and to believe that control will somehow deal with them. As shown for the reactive distillation example, however, standard methods may fail, especially if a process is run at an optimal point, because near such an operating point, some variables will exhibit a change of the sign of the gain unless the optimum is only defined by constraints. A combination of first principles-based and black box models, the parameters of which are estimated from operational data, may be a way to obtain sufficiently accurate models without excessive effort. In combination with this approach the application of optimization techniques which take model mismatch explicitly into account, as presented in Section 4.4, is very promising.

References

1 *Agreda V. H. Partin L. R. Heise W. H.* High purity methyl acetate via reactive distillation, Chem. Eng. Prog. 86 (1990) p. 40–46

2 *Altenhöner U. Meurer M. Strube J. Schmidt-Traub H.* Parameter estimation for the simulation of liquid chromatography, J. Chromatogr A 769 (1997) p. 59–69

3 *Brdyś M. Chen S. Roberts P. D.* An extension to the modified two-step algorithm for steady-state system optimization and parameter estimation, Int. J. Syst. Sci. 17 (1986) p. 1229–1243

4 *Brdyś M. Ellis J. E. Roberts P. D.* Augmented integrated system optimization and parameter estimation technique: derivation, optimality and convergence, IEEE Proc. 134 (1987) p. 201–209

5 *Brdyś M. Tajewski P.* An algorithm for steady-state optimizing dual control of uncertain plants, Proceedings of the 1st IFAC Workshop on New Trends in Design of Control Systems, Slovakia, (1994) pp. 249–254

6 *Broughton D.* (1966) Continuous simulated counter-current sorption process employing desorbent made in said process. US Patent 3.291.726

7 *Byrd R. H. Lu P. Nocedal J. Zhu C.* (1994) A limited memory algorithm for bound constrained optimization, Technical Report NAM-08, Department of Electrical Engineering and Computer Science, Northwestern University, USA

8 *Draeger A. Ranke H Engell S.* Model predictive control using neural networks. IEEE Control Syst. Mag. 15 (5) (1995) p. 61–66

9 *Dünnebier G. Engell S. Epping A. Hanisch F. Jupke A. Klatt K.-U. Schmidt-Traub H.* Model-based control of batch chromatography, AIChE J. 47 (2001) p. 2493–2502

10 *Dünnebier G. Klatt K.-U.* Modelling and simulation of nonlinear chromatographic separation processes: a comparison of different modelling approaches, Chem. Eng. Sci. 55 (2000) p. 373–380

11 *Engell S. Fernholz G.* Control of a Reactive Separation Process, Chem. Eng. Process. 42 (2003) p. 201–210

12 *Engell S. Müller R.* Multivariable controller design by frequency response approximation, Proceedings of the 2nd European Control Conference ECC2, Groningen, (1993) pp. 1715–1720

13 *Fernholz G. Engell S. Fougner K.* (1999a) Dynamics and Control of a Semibatch Reactive Distillation Process. Proc. 2nd European Congress on Chemical Engineering (CD-ROM), Montpellier

14 *Fernholz G. Engell S. Kreul L.-U. Górak A.* (2000) Optimal Operation of a Semibatch Reactive Distillation Column. Proc. 7th Int. Symposium on Process Systems Engineering, Keystone, Colorado. In: Computers & Chemical Engg. 24, 1569–1575

15 *Fernholz. G. Wang W. Engell S. Fougner K. Bredehöft J.-P.* Operation and control of a semi-batch reactive distillation column. Proceedings of the 1999 IEEE CCA, Kohala Coast, Hawaii, August 22–27, (1999b) pp. 397–402, IEEE Press

16 *Gao W. Engell S.* (2005) Iterative Set-Point Optimization of Batch Chromatography, *Computers and Chemical Engineering* 29, 1401–1410

17 *gPROMS User's Guide* (1997) Process System Enterprise, London, United Kingdom

18 *Gu T.* (1995) Mathematical Modelling and Scale Up of Liquid Chromatography, Springer, New York

19 *Guest D. W.* Evaluation of simulated moving bed chromatography for pharmaceutical process development, J.Chromatogr. A 760 (1997) p. 159–162

20 *Guiochon G.* Preparative liquid chromatography, J.Chromatogr. A 965 (2002) p. 129–161

21 *Hanisch F.* (2002) Prozessführung präparativer Chromatographieverfahren (Operation of Preparative Chromatographic Processes), Dr.-Ing. dissertation, University of Dortmund, and Shaker Verlag, Aachen (in German)

22 *Hotier G. Nicoud R. M.* (1996) Chromatographic simulated mobile bed separation process with dead volume correction using period desynchronization. US Patent 5 578 215

23 *Juza M. Mazzotti M. Morbidelli M.* Simulated moving-bed chromatography and its application to chirotechnology, Trends Biotechnol. 18 (2000) p. 108–118

24 *Klatt K.-U. Hanisch F. Dünnebier G.* Model-based control of a simulated moving bed chromatographic process for the separation of fructose and glucose, J. Process Control 12 (2002) p. 203–219

25 *Klatt K.-U. Dünnebier G. Hanisch F. Engell S.* (2002) Optimal Operation and Control of Simulated Moving Bed Chromatography: A Model-based Approach. *Invited Plenary Paper*, CACHE/AIChE Conference Chemical Process Control 6, 2001, Tucson. In: J. B. Rawlings, B. A. Ogunnaike, and J. W. Eaton (Eds.): *Chemical Process Control VI*, AIChE Symposium Series No. 326, Vol. 98 CACHE Publications, 2002, 239–254

26 *Kreul L. U. Górak A. Dittrich C. Barton P. I.* Dynamic catalytic distillation: advanced simulation and experimental validation, Comput. Chem. Eng. 22 (1998) p. 371–378

27 *Lin J. C. Han P. D. Roberts P. D. Wan B. W.* New approach to stochastic optimizing control of steady-state systems using dynamic information, Int. J. Control 50 (1989) p. 2205–2235

28 *Máckowiak J.* (1991) Fluiddynamik von Kolonnen mit modernen Füllkörpern und Packungen für Gas-/Flüssigsysteme, 1. Auflage, Otto-Salle-Verlag, Frankfurt (in German)

29 *Nagrath D. Bequette B. Cramer S.* Evolutionary operation and control of chromatographic processes, AIChE J. 49 (2003) p. 82–95

30 *Noeres C.* (2003) Catalytic distillation: dynamic modelling, simulation and experimental validation, Dr.-Ing. dissertation, University of Dortmund, and VDI Verlag, Düsseldorf

31 *Roberts P. D.* An algorithm for steady-state system optimization and parameter estimation, Int. J. Syst. Sci. 10 (1979) p. 719–734

32 *Roberts P. D.* Broyden derivative approximation in ISOPE optimizing and optimal control algorithms, Proceedings of the 11th IFAC Workshop on Control Applications of Optimization CAO'2000, Elsevier (2000) pp. 283–288

33 *Tatjewski P.* (2002) Iterative optimizing set-point control – the basic principle redesigned, Proceedings of the 15th Triennial IFAC World Congress, CD-ROM, Barcelona

34 *Tatjewski P. Brdyś M. A. Duda J.* Optimizing control of uncertain plants with constrained feedback controlled outputs, Int. J. Control 74 (2001) p. 1510–1526

35 *Toumi A. Engell S.* (2004c) A software package for optimal operation of continuous moving bed chromatographic processes. In: H. G. Bock, E. Kostina, H. X. Phu, and R. Rannacher (Eds.): *Modelling Simulation and Optimization of Complex Processes (Proceedings of the International Conference on High Performance Scientific Computing, Hanoi, 2003)*, Springer, 471–484

36 *Toumi A. Engell S.* Optimal operation and control of a reactive simulated moving bed process, Proceedings of the IFAC Symposium on Advanced Control of Chemical Processes, Hong Kong, Elsevier (2004a) pp. 243–248

37 *Toumi A. Engell S.* (2004b) Optimization-based Control of a Reactive Simulated Moving Bed Process for Glucose Isomerization, Chemical *Engineering Science* 59, 3777–3792

38 *Toumi A. Engell S.* (2005) Advanced control of simulated moving bed processes. In: H. Schmidt-Traub (Ed.): *Preparative Chromatography of fine chemicals and pharmaceuticals agents*, Wiley-VCH, Weinheim.

39 *Toumi A. Engell S. Ludemann-Hombourger O. Nicoud R. M. Bailly M.* Optimization of simulated moving bed and VARICOL processes, J.Chromatogr. A 1006 (2003) p. 15–31

40 *Wang C. Klatt K. Dünnebier G. Engell S. Hanisch F.* Neural network based identification of SMB chromatographic processes, Control Eng. Practice 11 (2003) p. 949–959

41 *Zhang Z. Mazzotti M. Morbidelli M.* Power-Feed operation of simulated moving bed units: changing flow-rates during the switching interval, J. Chromatogr. A 1006 (2003) p. 87–99

42 *Zhang H. Roberts P. D.* On-line steady-state optimization of nonlinear constrained processes with slow dynamics, Trans. Inst. Measure. Control. 12 (1990) p. 251–261

43 *Zhou J. L. Tits A. L. Lawrence C. T.* (1997) User's Guide for FFSQP Version 3.7: a FORTRAN code for solving constrained nonlinear (minimax). optimization problems, generating iterates satisfaying all inequality and linear constraints, University of Maryland